Effect of torso morphology on maximum hydrodynamic resistance in front crawl swimming

Effect of torso morphology on maximum hydrodynamic resistance in front crawl swimming

Christopher Papic [a]*, Carla McCabe[b], Tomohiro Gonjo[c] and Ross Sanders[a]

[a] *Exercise and Sport Science, Faculty of Medicine and Health, The University of Sydney, Sydney, Australia*

[b] *School of Sport, Faculty of Life and Health Sciences, Ulster University, Jordanstown, Northern Ireland*

[c] *Department of Physical Performance, Norwegian School of Sport Sciences, Oslo, Norway*

*corresponding author

Mailing address: U3 69 Beaconsfield Street, Newport, 2106 (NSW, Australia)

P: +61 421 519 172

E: chris.papic@sydney.edu.au

Twitter: @chris_papic

Effect of torso morphology on maximum hydrodynamic resistance in front crawl swimming

The aim of this study was to determine the influence of torso morphology on maximum instantaneous hydrodynamic resistance in front crawl swimming. Outlines of the torso in the frontal and anteroposterior planes were calculated from photographic images to determine continuous form gradients (m/m) for the anterior, posterior and lateral aspects of the torso. Torso cross-sectional areas at each vertical sample (0.001m) were used to calculate maximal rate of change in cross-sectional area (m^2/m^1) in the chest-waist and waist-hip segments. During catch-up arm coordination in middle-long distance front crawl swimming, kicking propulsion is negligible and therefore the net force is equal to the drag during the non-propulsive hand phase. Drag coefficients were calculated at the instant of maximum horizontal deceleration of centre of mass during the non-propulsive hand phase of 400m pace front crawl stroke cycles. Maximal rate of change in cross-sectional area (r=0.44, p=0.014) and posterior form gradient (r=0.50, p=0.006) of the waist-hip torso segment had moderate positive correlations with the coefficient of drag. A regression model including these two variables explained 41% of the variance (p=0.001). Indentation at the waist and curvature of the buttocks may result in greater drag force and influence swimming performance.

Keywords: anthropometry, drag coefficient, fluid dynamics, swimming performance

Introduction

The velocity of a human swimmer is determined by the interaction between propulsion developed actively by muscular contractions and resistive forces (hydrodynamic resistance) associated with movement of the body through water (Benjanuvatra, Blanksby, & Elliott, 2001; Pendergast et al., 2005). Understanding the relationship between body morphology and hydrodynamic resistance is important to identify differences in natural attributes of swimmers that affect their potential to succeed at a high level. Quantifying hydrodynamic resistance encountered by a swimmer is an ongoing challenge for researchers. Active drag, that is, the hydrodynamic resistance while swimming with stroking and kicking actions, has been estimated by various methods including the Measurement of Active Drag (MAD) system (Hollander et al., 1986). The MAD system is based on the assumption that at constant average velocity across stroke cycles the net impulse for a single stroke cycle is zero and therefore the propulsive and hydrodynamic resistive impulses are equal in magnitude (Van der Vaart et al., 1987). However, swimmers' velocities fluctuate throughout the front crawl stroke cycle due to the various propulsive and recovery phases (Alcock & Mason, 2007; Psycharakis, Naemi, Connaboy, McCabe, & Sanders, 2010) making it difficult to quantify the actual instantaneous drag forces to assess the effect of body shape characteristics on hydrodynamic resistance.

Hydrodynamic resistance brought about by the arms during the front crawl stroke cycle is the lowest in magnitude during the non-propulsive hand phase, with one arm outstretched in front of the swimmer preparing for the 'catch' and the other arm above the water surface (Gatta, Cortesi, Fantozzi, & Zamparo, 2015). This arm coordination is known as 'catch-up' and is commonly exhibited by swimmers during middle- and long-distance front crawl swimming (Seifert, Chollet, & Bardy, 2004). Assuming that the propulsive force due to the kick is negligible, the net force during this period of the stroke

cycle is affected only by hydrodynamic resistance. Consequently, the magnitude of deceleration of the swimmer during the non-propulsive hand phase provides an opportunity to assess the effects of the swimmer's morphology on hydrodynamic resistance.

With respect to human swimming, fluid flow may separate from the boundary layer, the layer of fluid flow in contact with the body, due to the morphology of the swimmer (Mollendorf, Albert, Oppenheim, & Pendergast, 2004). This separation from the boundary layer creates turbulent flow and a resulting pressure differential causing increased form drag (Marinho, Barbosa, Rouboa, & Silva, 2011), the drag produced from the physical characteristics of the body (Hertel, 1966). Marine animals exhibit body shape characteristics that minimise hydrodynamic resistance. One characteristic that aids dolphins in minimising form drag is a low rate of change in cross-sectional area (CSA) when progressing caudally (Fish & Hui, 1991). Furthermore, the form gradient, the rate of change in the body outline in the frontal and anteroposterior planes, is gradual without sudden changes in curvature. A low rate of change in CSA and a low form gradient minimises turbulence and disruption to fluid flow around the body than a high rate of change. Morphological characteristics that minimise turbulence along a body are advantageous for reducing hydrodynamic resistance. There is an assumption that areas of the human torso such as the indentation of the waist and curvature of the buttocks may have rapid changes in curvature when compared with dolphins, which may disrupt fluid flow around the body when moving through the water.

Analysis of the effects of torso morphology on hydrodynamic resistance and performance has focused predominantly on singular anthropometric measures; breadths, circumferences and CSA (Benjanuvatra et al., 2001; Lyttle, Blanksby, Elliot, & Lloyd, 1998). In relation to swimming humans, 'projected frontal area' or 'trunk transverse

surface area' (TTSA) refers to the largest CSA of the swimmer in the transverse plane of the body. TTSA has been calculated using the planimetric method from 2D digital images in the transverse plane taken above the swimmer whilst on land (Morais et al., 2011; Vilas-Boas et al., 2010) and from the frontal view of a swimmer during free-swimming and underwater mono-fin swimming (Gatta et al., 2015; Nicolas, Bideau, Colobert, & Berton, 2007). Male swimmers have been shown to have larger active drag and drag coefficient values than female swimmers during front crawl swimming without kicking actions, which has been attributed to a larger TTSA (Toussaint et al., 1988). TTSA in the transverse plane with two arms extended above the head was found to have a high positive correlation with the coefficient of drag during front crawl swimming without kicking actions (r=0.87) (Huijing et al., 1988). TTSA considers additional body segments that protrude beyond the chest CSA in the transverse plane, such as the shoulders and hips, that can increase hydrodynamic resistance. While a relationship has been found between TTSA and hydrodynamic resistance in front crawl, TTSA represents a 2D image and therefore does not consider curvatures along the torso or the site in which curvatures and indentations reside that may influence hydrodynamic resistance. Mollendorf et al. (2004) proposed that significant changes in curvature along the body may result in fluid flow separation and the subsequent turbulence and pressure differentials.

While there is some evidence that morphological characteristics of the torso affect hydrodynamic resistance, singular measures do not consider the effect of shape variations along the length of the torso that influence fluid flow and hydrodynamic resistance. The aim of this study was to determine the influence of torso morphology on maximum instantaneous hydrodynamic resistance in front crawl swimming. It was hypothesised that the rate of change in CSA and form gradient when progressing caudally along the torso would be associated with hydrodynamic resistance during front crawl swimming.

Knowledge of morphological characteristics of the torso that minimise hydrodynamic resistance may be useful for identifying talent, manipulating swimming technique and for optimising body shape through strength and conditioning, swimming training, and nutritional strategies.

Methods

Participants

Photographic imaging and whole-body centre of mass data sets of male swimmers were used from studies conducted by McCabe and Sanders (2012) at the Centre for Aquatics Research and Education (CARE), The University of Edinburgh, and Gonjo et al. (2019) at the Aquatics Research Centre at the University of Porto. These were defined as Group 1 and Group 2, respectively. These data sets were used as the methods of data collection and quantification of whole-body centre of mass were consistent. Group 1 included 15 Scottish national and international level male swimmers; seven sprint specialists (18.3±2.3years, 75.8±6.4kg, 184.4±6.3cm, 400m front crawl swim time 4.24.2mins±9.10sec, 50m front crawl swim time less than 24.60sec) and eight distance specialists (17.5±2.5years, 72.3±10.5kg, 181.8±7.5cm, 400m front crawl swim time 4.02.59min±7.08 s) (McCabe & Sanders, 2012). Group 2 included ten male national level Portuguese swimmers (17.47±1.00years; 70.05±6.63 kg; 179.14±5.43cm, 100m front crawl swim time 54.50±1.23sec) (Gonjo et al., 2019). Despite differences in event speciality, no kinematic differences were found between the sprint and distance specialist swimmers at 400m front crawl swimming pace (McCabe & Sanders, 2012). Testing procedures were approved by the relevant institutional ethics committees and all swimmers provided written informed consent to participate in the study.

Experimental design

Photographic imaging

Photographic images of the swimmers were obtained for two purposes. The first was to enable body segment parameters to be determined by the Elliptical Zone Method for subsequent calculation of each participant's centre of mass position (Deffeyes & Sanders, 2005). The second was to enable the contours of the torso to be traced for subsequent analysis of the effect of torso shape on the drag coefficient. Swimmers in Group 1 and Group 2 were marked with black circular marks (Grimas Créme Make Up) on nineteen anatomical landmarks for the calculation of centre of mass: the vertex of the head, the right and left of the: tip of the third distal phalanx of the finger, wrist axis, elbow axis, shoulder axis, hip axis, knee axis, ankle axis, fifth metatarsophalangeal joint, and the tip of the first phalanx (Deffeyes & Sanders, 2005). Two digital cameras, Nikon E4200 (Minato, Tokyo, Japan) and Canon Ixus 400 (Ōta, Tokyo, Japan) were positioned on tripods at a height of 1.0m with their axis aligned horizontally and perpendicular to the swimmers' frontal and anteroposterior planes. The swimmers were photographed in the anatomical position wearing regular swimming trunks to facilitate valid comparison of body shape characteristics between swimmers. In both the anterior and lateral images, the swimmer's arms were positioned such that the outline of the torso was visible for tracing.

Data collection and processing

Swimmers completed an individual warm-up consisting of stretching, front crawl swimming and swimming drills. Swimmers in Group 1 performed a maximal evenly paced 400m front crawl swim through a 6.75m^3 calibrated space. Swimmers in Group 2 performed a 50m front crawl swimming trial at 400m front crawl swimming velocity through a 30.0m^3 calibrated space. The swimmers were recorded by four above and two

below water JVC KY32 CCD (Long Beach, California, USA) cameras for Group 1 and HDR-CX160E (Tokyo, Japan) cameras for Group 2. The cameras were synchronised and recorded at 50Hz. A single stroke cycle was captured in the middle of the pool during each 50m segment of the 400m trial for swimmers in Group 1. To facilitate valid within-participant comparison in the current study, laps 1 and 6–8 were removed to negate the influence of greater swimming velocities in lap 1 than the remainder of the 400m trial and the fatigue effect in laps 6–8. Thus, a total of four captured stroke cycles were analysed per swimmer corresponding to laps 2–5. A single stroke cycle was captured in the middle of the pool during the 50m trial of swimmers in Group 2.

All swimmers were instructed to not breathe during the captured stroke cycle. This minimised possible confounding of drag coefficients by breathing technique and the associated lateral body movements, as lateral body movements are found to increase hydrodynamic resistance (Zamparo, Gatta, Pendergast, & Capelli, 2009). Nineteen anatomical landmarks on the participants were manually digitised, by the same operator, for each video frame using APAS (Ariel Dynamics Inc., San Diego, USA) for the above and below water fields of view prior to calculation of three-dimensional (3D) coordinates by the APAS direct linear transformation process. Digitising reliability was found to be acceptable with small reported errors in mean centre of mass velocity (m/s, SD=0.01, coefficient of variation=0.22) after digitising a single stroke cycle ten times by the same operator (McCabe, Psycharakis, & Sanders, 2011). The 3D coordinates and the body segment parameter data were then input to a bespoke MATLAB program (Mathworks Inc., Massachusetts, USA) to calculate centre of mass position. The centres of mass coordinates were interpolated using Fourier transform and inverse transform to 201 points (Group 1) representing half percentiles of the stroke cycle, and 101 points (Group 2) representing percentiles of the stroke cycle. A stroke cycle was defined as the instant of

entry of one hand to the instant of re-entry of the same hand. Instantaneous horizontal velocities (v, m/s) and accelerations (α, m/s^2) of centre of mass were derived for each sample (i) of the *x* (swimming direction) coordinate of the centre of mass displacement (*x*, m) data using Equation 1 and Equation 2, respectively. Initial coordinate data filtering (4th Order Butterworth with a cut off frequency of 6Hz) ensured that the minimum and maximum velocity and acceleration peaks identified from the derived time series were not inflated by noise.

$$\mathrm{v}\,(i) = \frac{x(i+1)-x(i-1)}{t(i+1)-t(i-1)} \quad (1)$$

$$\alpha\,(i) = \frac{x(i+1)-2x(i)+x(i-1)}{[t(i+1)-t(i)]^2} \quad (2)$$

Torso shape analysis

The photographic images were input into the bespoke MATLAB program 'TorsoShape' adapted from the 'eZone' program (Deffeyes & Sanders, 2005) as described by Papic et al. (2019). Calibration for the front and side views involved digitising images of the calibration frame for five control markers in the X-axis spaced 0.2m apart and six control markers in the Y-axis spaced 0.2m apart. A single operator then traced, using a mouse and cursor, the outlines of the torso from the front and side views. The tracings extended beyond the C7 and greater trochanter landmarks to eliminate endpoint distortion in subsequent low-pass filtering. A zoom function ensured accuracy during the calibration and tracing of the swimmer's torso. The program interpolates the sampled points to yield the two-dimensional coordinates of the tracings with the vertical (Z) coordinates being 1mm apart, smooths the data at 12Hz using a Butterworth 4th order digital filter and aligns the 1mm samples of the four tracings to a common vertical reference. The program automatically outputs the coordinates of each tracing for the frontal plane (X, Z) and for the anteroposterior plane (Y, Z) and the difference between the X coordinates at each Z sample and the Y coordinates at each Z sample.

Cross-sectional area

The torso was modelled as a series of vertically stacked ellipses (Jensen, 1978) at 1 mm increments using the differences in X and Y coordinates as the diameters of each ellipse. Transverse and anteroposterior diameters are initially converted to radii (a and b, respectively). The area of an ellipse formula (CSA = πab) was used to estimate CSAs moving caudally along the torso. The largest CSA between C7 vertebrae height and the waist was defined as 'chest CSA' (m^2), the smallest CSA as 'waist CSA' and the CSA at the greater trochanter as 'hip CSA'.

Rate of change in cross-sectional area

Previous research compared the maximal rate of change in CSA between a male and female mannequin (Pease & Vennell, 2011). Using Microsoft Excel (Microsoft Corp., Washington, USA), the change of the CSA values between adjacent vertical increments (0.001m) were calculated using the central difference formula and represented the rate of change in CSA moving caudally along the swimmer's torso. The greatest rate of change in CSA between chest-waist and waist-hip (m^2/m) was calculated for each segment. A negative rate of change indicates that CSA is reducing when progressing caudally, whilst a positive value indicates that CSA is increasing.

Form gradients

Form gradients indicated the 'suddenness' of body shape change in the swimmer's body outline in the frontal and anteroposterior planes. The maximum form gradient (m/m) of the left and right lateral aspects of the torso in the frontal plane (X, Z) and anterior and posterior aspects of the torso in the anteroposterior plane (Y, Z) were calculated in Microsoft Excel from the coordinate values of the swimmer's torso outline using the first central difference formulae; Equation 3 and Equation 4, respectively. Each form gradient

was separated into chest-waist and waist-hip segments to assess change in curvature between the points at which the CSAs were maximum at the chest and hips and minimum at the waist (Figure 1). For the side and front camera views of the torso, a negative form gradient indicated that the portion of the torso was sloping inwards with respect to the longitudinal axis, whilst a positive form gradient indicated that the torso was sloping outwards with respect to the longitudinal axis.

$$\mathrm{FG}_{\mathrm{Frontal}}\,(i) = \frac{X(i+1)-X(i-1)}{Z(i+1)-Z(i-1)} \quad (3)$$

$$\mathrm{FG}_{\mathrm{Anteroposterior}}\,(i) = \frac{Y(i+1)-Y(i-1)}{Z(i+1)-Z(i-1)} \quad (4)$$

Figure 1. Maximum segment form gradient (m/m): Lateral (right) chest-waist (1–3) and waist-hip (3–5), lateral (left) chest-waist (2–4) and waist-hip (4–6), posterior chest-waist (7–9) and waist-hip (9–11), anterior chest-waist (8–10) and waist-hip (10–12).

Coefficient of drag

The coefficient of drag is commonly used as an indicator of the influence of the shape characteristics of a body on hydrodynamic resistance. As such, it is useful to explain differences in swimming performance (Havriluk, 2005). The estimate of the coefficient of active drag can be obtained if the resistive force, water density, cross sectional area, and velocity are known. However, as is the case with the estimate of active drag it is generally based on the drag experienced during a whole stroke cycle or several stroke cycles and therefore represents a mean value despite periods of acceleration and deceleration in the stroke cycle. One of the few studies to obtain a coefficient corresponding to particular events involving deceleration of the swimmer was conducted by Vilas-Boas et al. (2010). They obtained a coefficient of drag during the first and second

gliding positions of the underwater breaststroke stroke following the dive or turn using deceleration force derived by inverse dynamics. Similarly, Morais et al. (2013) obtained coefficients of swimmers during underwater gliding in a static streamlined body position. While the net deceleration force in the breaststroke and streamlined gliding positions are equal to the resistive force, a conceptual approach similar to those studies can be applied to the catch-up portion of the front crawl stroke cycle where propulsive force from kicking is negligible.

The coefficient of drag force in the current study was determined by rearranging the equation embodying Newton's second law of motion to obtain the total drag force (Equation 5). The maximum coefficient of drag (C_d), at the time swimmers did not perform propulsive upper-limb motion, was obtained from Equation 6 with values input for the swimmer's total mass (m) (body mass and added fluid mass) (Morais et al., 2013), maximal CSA (A), velocity (v), acceleration (α) and fluid density (ρ) (1000 kg/m^3). Total mass was calculated as body mass (kg) multiplied by 1.268, as male swimmers have been found to have an average added mass of 26.8% (Caspersen, Berthelsen, Eik, Pâkozdi, & Kjendlie, 2010). Added mass is the mass of fluid moving in conjunction with the body, including the boundary layer (Naemi & Sanders, 2008). Previous research supports the use of maximal CSA to substitute for A and a power of two for swimming velocity (Havriluk, 2005). An instantaneous measure of maximum deceleration (m/s^2) during the non-propulsive hand phase defined the acceleration term (α) of Equation 6. The drag coefficient derived for each of the four stroke cycles per swimmer in Group 1 were averaged to represent a mean drag coefficient for each swimmer.

$$\mathrm{F}d = m \cdot \alpha = \frac{1}{2} \cdot Cd \cdot \rho \cdot A \cdot \mathrm{v}^{\mathrm{n}} \qquad (5)$$

$$Cd = \left|\frac{(m \cdot \alpha \cdot 2)}{(\rho \cdot A \cdot v^2)}\right| \quad (6)$$

Statistical analysis

Statistical analysis was performed using SPSS software (Version 25, SPSS Inc., Chicago, USA). Independent sample Welch's T-tests were performed between Group 1 and Group 2 for torso shape measurements and drag coefficients to determine whether differences existed between the two sample sets. If no differences existed between the groups, the groups would be combined to increase the sample size. Pearson correlation coefficients were calculated to determine the influence of each torso shape measure on the coefficient of drag. Pearson correlation coefficient strength of association was defined by the following criteria: r=0–0.19 as very weak, r=0.2–0.39 as weak, r=0.40–0.59 as moderate, r=0.60–0.79 as strong and r=0.8–1.0 as very strong (Evans, 1996). A stepwise linear regression analysis was conducted using the SPSS linear regression 'step-wise' function, to determine the relationship of torso shape measures and the coefficient of drag during front crawl swimming. The 'bootstrap' statistical function for linear regressions in SPSS was conducted with 2000 bootstrap sample iterations on significant predictors of the drag coefficient. Bootstrapping is a non-parametric data resampling technique that retrieves random samples from the total data set and estimates the indirect effects in each resampled data set (MacKinnon, Lockwood, & Williams, 2004). Bootstrapping is used to improve the accuracy of statistical estimations (Juan & Lantz, 2001). Bootstrapping was used to derive bias-corrected and accelerated 95% confidence intervals for Pearson correlation coefficients and the statistical significance of predictors in the regression model. Statistical significance was accepted at p<0.05.

Results

Mean torso shape measures and drag coefficient values for the two data sets (Group 1 and Group 2) and the combined cohort are reported in Table 1. There were no significant differences in torso morphology and coefficient of drag values between Group 1 and Group 2. Consequently, Group 1 and Group 2 were pooled together as a combined cohort of swimmers (n=25) to determine the influence of torso morphology on the coefficient of drag.

Table 1. Mean (standard deviation) torso shape and drag coefficient measurements for Group 1, Group 2 and Combined Cohort.

Significant moderate positive correlations were found between rate of change in CSA (r=0.44, p=0.014; 95% CI=0.16, 0.69) and the posterior form gradient waist-hip (r=0.50, p=0.006; 95% CI=0.15, 0.74) with the drag coefficient. The two torso shape measurements and their relationship with the drag coefficient are independently expressed in Figure 2 and Figure 3 with their respective Pearson correlation coefficients. Table 2 summarises the Pearson correlation coefficients for all torso shape measurements and their influence on the drag coefficient. Using the stepwise regression method it was found that the rate of change in CSA waist-hip (β=0.46, p=0.007) and the posterior form gradient waist-hip (β=0.52, p=0.003) were significant predictors of the coefficient of drag during front crawl swimming, explaining 41% of the variance (*adjusted* R^2=0.41, p=0.001*)*. The linear regression bootstrapping procedure, with 2000 bootstrap resample iterations, revealed that the rate of change in CSA waist-hip (p=0.009) and posterior form gradient waist-hip (p=0.001) were still significant predictors of maximal drag coefficients in front crawl swimming.

Table 2. Pearson correlation coefficient between torso shape measurements and the drag coefficient (n=25).

Figure 2. Maximum rate of change in cross sectional area waist-hip vs maximum drag coefficient.

Figure 3. Maximum posterior form gradient waist-hip vs maximum drag coefficient.

Discussion and implications

This study quantified the rate of change in CSA and the form gradients of the anterior, posterior and lateral aspects of the torso to determine the relationship between torso morphology and an instantaneous drag coefficient during front crawl swimming. It was hypothesised that a relationship would exist between the rate of change in CSA and hydrodynamic resistance and form gradient of the torso and hydrodynamic resistance during front crawl swimming. In support of the hypothesis, maximum rate of change in CSA waist-hip and posterior form gradient waist-hip had moderate positive correlations with the drag coefficient, accounting for 41% of variance when combined in the regression equation. A high rate of change in CSA when progressing caudally from the waist and a greater posterior form gradient indicated a larger indentation at the waist and curvature of the buttocks, respectively.

While the causal mechanism of the relationship between rate of change in CSA and posterior form gradient on the coefficient of drag cannot be confirmed by the findings, previous research can give insight into the association between indentation at the waist and curvature of the hips with fluid flow. Pressure area analysis, using CFD, of a national level female swimmer's body was conducted during underwater gliding in the

streamlined horizontal body position (Beaumont, Taïar, & Polidori, 2017). It was found that the largest total pressure area (pascals) produced by fluid flow on the body was the head of the swimmer, whilst the arms, superior aspect of the buttocks and posterior aspects of the legs were the next significant pressure areas. The pressure area in the section from the lumbar region to the buttocks is of interest as it coincides with the posterior form gradient waist-hip segment analysed in the current study and supports Mollendorf et al. (2004) who hypothesised that fluid flow separation and the subsequent generation of turbulence and pressure differentials may occur along the body where there are significant changes in curvature. This implies that manipulating body positioning and stroke mechanics to minimise curvatures, such as excessive lordosis in the lower back region, may reduce hydrodynamic resistance.

In that vein, manipulation of torso morphology of one male international level swimmer has been achieved by wearing a whole-body swimsuit (Machtsiras, 2012). The use of a whole-body swimsuit had a significant effect on the glide factor, a measure of hydrodynamic efficiency of the body derived using the 'Hydro-Kinematic' method, of the male swimmer (d=3.317, p<0.001) (Naemi & Sanders, 2008). Improvements in the swimmer's glide factor by 16.7% when wearing the whole-body swimsuit were thought to be due to morphological changes to the swimmer's body (Machtsiras, 2012). These changes included a reduction in CSAs of the chest by 1.95% and the hips by 3.67%, whilst increasing the CSA of the waist by 8.21%, when comparing the whole-body swimsuit with the regular swimsuit (Machtsiras, 2012). Reducing chest and hip CSA, whilst increasing waist CSA would theoretically reduce the rate of change in CSA waist-hip and the posterior form gradient waist-hip of the swimmer. While whole-body swimsuits are currently banned in competitive swimming, their reduction in body CSAs and subsequent improvement in glide efficiency support the findings from the current study, whereby the

magnitude of curvature from waist-hip was associated with the hydrodynamic properties of the swimmer's body.

To our knowledge, this is the first study to quantify curvatures of the torso to assess their influence on hydrodynamic resistance. While Pease and Vennell (2011) investigated the rate of change in CSA of the body and referred to curvatures along the torsos of male and female mannequins, they did not calculate form gradients or an equivalent measure of the body outline. The advantage of calculating form gradients in the frontal and anteroposterior planes is that rate of change in CSA does not distinguish the shape characteristics or direction, with respect to the path of fluid flow, of body mass distribution along the torso. Swimmers of similar body mass and rate of change in CSA from waist-hip could have different form gradients representative of different curvatures produced by posture and body mass distribution around the lower abdomen, iliac crest or buttocks. For example, two swimmers from Group 1 had a body mass difference of 1.9% (74.8kg vs 76.2kg) and maximal rate of change in CSA waist-hip difference of 4.2% ($0.268 m^2/m$ vs $0.279 m^2/m$), but differed in their posterior form gradient waist-hip and drag coefficient values by 12.3 % (0.570m/m vs 0.640m/m) and 48.3% (2.40 and 3.56), respectively.

Instantaneous drag coefficients calculated in the current study from front crawl swimming were significantly greater than those derived from front crawl active drag analysis throughout the literature. The mean of drag coefficients derived in previous research from added and/or subtracted active drag methods, such as the velocity perturbation and assisted towing methods, was substantially less than our study at 1.59 (Havriluk, 2007). Differences in drag coefficients may be due to the assumption used in active drag methodologies, that a swimmer's velocity remains constant throughout the stroke cycle, rather than fluctuating. In studies that have determined drag coefficients

during underwater gliding using deceleration force of swimmers, drag coefficients were also calculated using a mean value of deceleration and velocity throughout the glide (Morais et al., 2013; Vilas-Boas et al., 2010). In contrast, the current study derived drag coefficients at the instant of maximum horizontal deceleration rather than a mean value representing the entire stroke cycle, which may explain the differences in drag coefficients between studies. Added and/or subtracted active drag methods may alter regular swimming technique as the swimmers are physically attached to a pulley system or towing a hydrodynamic buoy, manipulating the stimulus they are regularly exposed to. Swimmers in the current study performed front crawl swimming without changes to their regular swimming technique highlighting the utility of deriving an instantaneous maximum drag coefficient from the deceleration phase of the stroke cycle when assessing the influence of human morphology on the coefficient of drag.

Findings from the current study have implications for talent identification for middle-long distance front crawl swimming, where swimmers with optimal torso shapes may exhibit greater swimming efficiency than swimmers with greater body shape variability from waist-hip. A focus on improving swimming efficiency and optimising the hydrodynamic body position appears to be the most advantageous approach to improving swimming performance (Morais et al., 2012). Manipulation of front crawl technique to minimise excessive lordosis through the lumbar spine may reduce the posterior form gradient from waist-hip and subsequent fluid flow deviation. For example, feedback and cuing of swimmers to actively engage gluteal muscles during front crawl may assist in maintaining neutral pelvic alignment and minimise hip curvature. Improvements in hydrodynamic resistance have been achieved previously by providing feedback and cuing to manipulate swimmers' posture during underwater gliding (Thow, Naemi, & Sanders, 2012) .

Manipulation of torso morphology has been evident in the design of competitive swimsuits. While the Swimwear Approval Committee of FINA assesses competitive swimsuits with specific guidelines on the material makeup and characteristics of the swimsuit (e.g. thickness, buoyancy and permeability), investigating the effect of new swimsuits on body curvatures and the subsequent hydrodynamic resistance ought to be considered, especially for female swimsuits that cover the chest, waist and hips. Other than using swimsuits, body sculpting through training and nutritional strategies may be implemented to improve hydrodynamic shape. However, researchers carrying out this approach would need to consider how changes in body shape may alter the power to weight ratio of the swimmer. Further investigations involving male and female swimmers would be advantageous to investigate whether differences in body shape exist between sexes and the potential influence that different body contours and curvatures have on hydrodynamic resistance.

The current study has several limitations that ought to be considered when interpreting the findings. Body shape influences the mass of fluid moving in conjunction with the body (Caspersen et al., 2010), thereby affecting inertia and the magnitude of deceleration (Naemi & Sanders, 2008). While maximum deceleration of the body was used to calculate the drag coefficient in our study, the maximum instantaneous force was based partly on an estimate of added mass rather than a known value. As a consequence, the effect of torso shape on added mass and the drag coefficient could not be measured directly. Waist-hip morphology during the static standing body position is comparable to the body position during the non-propulsive hand phase of front crawl swimming. Morphological differences, however, may occur between the static standing and non-propulsive hand phase body positions, as the chest-waist segment may be manipulated when the arms are outstretched above the head. Deriving torso curvatures and

indentations from underwater images of the swimmer at key instances throughout the stroke cycle in future research would be advantageous to further our understanding of the hydrodynamic profile of human swimmers. Furthermore, results from the bootstrapping statistical method revealed that the 95% confidence intervals of Pearson correlation coefficients ranged from ‘weak’ to ‘strong’ for both predictors of the drag coefficient; rate of change in CSA waist-hip and posterior form gradient waist-hip. Further research involving larger sample sizes would be advantageous to improve the accuracy of the relationship magnitude between waist-hip morphology and the drag coefficient.

Conclusions

Preliminary findings have shown that a significant relationship exists between the rate of change in shape from the waist to the hip and the coefficient of drag. Greater indentation at the waist and ‘bulge’ of the buttocks may result in deviation to fluid flow and turbulence in the lumbar region of the swimmer’s posterior aspect that result in increased hydrodynamic resistance. The method of quantifying torso shape described in this paper will be applied in further investigations to determine the influence of torso curvatures and shape, of male and female swimmers, on glide efficiency, to develop an understanding of how performance in the underwater glide phase of swimming can be improved.

Acknowledgements

We would like to thank Professors Joao Paulo Vilas-Boas and Ricardo Fernandes and their research team at the University of Porto, Portugal, for their contributions in recruiting swimmers and facilitating data collection at that venue.

460 **References**

461 Alcock, A., & Mason, B. (2007). Biomechanical analysis of active drag in swimming.
462 *Proceedings of XXV International Symposium on Biomechanics in Sports*, Ouro
463 Preto, Brazil, 212-215.
464 Beaumont, F., Taïar, R., & Polidori, G. (2017). Preliminary numerical investigation in
465 open currents-water swimming: Pressure field in the swimmer wake. *Applied*
466 *Mathematics and Computation, 302*, 48-57.
467 Benjanuvatra, N., Blanksby, B. A., & Elliott, B. C. (2001). Morphology and
468 hydrodynamic resistance in young swimmers. *Pediatric Exercise Science, 13*(3),
469 246-255.
470 Caspersen, C., Berthelsen, P. A., Eik, M., Pâkozdi, C., & Kjendlie, P-L. (2010). Added
471 mass in human swimmers: age and gender differences. *Journal of Biomechanics*,
472 *43*(12), 2369-2373.
473 Deffeyes, J., & Sanders, R. (2005). Elliptical zone body segment modellng software:
474 digitising, modellng and body segment parameter calculation. *Proceedings of*
475 *XXIII International Symposium on Biomechanics in Sports*, Beijing, China, 749-
476 752.
477 Evans, J. D. (1996). *Straightforward statistics for the behavioral sciences*. Pacific Grove:
478 Thomson Brooks/Cole Publishing Co.
479 Fish, F. E., & Hui, C. A. (1991). Dolphin swimming–a review. *Mammal Review, 21*(4),
480 181-195.
481 Gatta, G., Cortesi, M., Fantozzi, S., & Zamparo, P. (2015). Planimetric frontal area in the
482 four swimming strokes: Implications for drag, energetics and speed. *Human*
483 *movement science, 39*, 41-54.
484 Gonjo, T., McCabe, C., Coleman, S., Soares, S., Fernandes, R. J., Vilas-Boas, J. P., &
485 Sanders, R. (2019). Do swimmers conform to criterion speed during pace-

controlled swimming in a 25-m pool using a visual light pacer? *Sports biomechanics*, 1-14.

Havriluk, R. (2005). Performance level differences in swimming: a meta-analysis of passive drag force. *Research quarterly for exercise and sport, 76*(2), 112-118.

Havriluk, R. (2007). Variability in measurement of swimming forces: a meta-analysis of passive and active drag. *Research quarterly for exercise and sport, 78*(2), 32-39.

Hertel, H. (1966). *Structure, form, movement*. New York: Reinhold.

Hollander, A., De Groot, G., van Ingen Schenau, G., Toussaint, H., De Best, H., Peeters, W., . . . Schreurs, A. (1986). Measurement of active drag during crawl arm stroke swimming. *Journal of sports sciences, 4*(1), 21-30.

Huijing, P., Toussaint, H., Mackay, R., Vervoon, K., Clarys, J., & Hollander, A. (1988). Active drag related to body dimensions. *Swimming science V, 18*, 31-37.

Jensen, R. K. (1978). Estimation of the biomechanical properties of three body types using a photogrammetric method. *Journal of biomechanics, 11*(8-9), 349-358.

Juan, S., & Lantz, F. (2001). Application of bootstrap techniques in econometrics: the example of cost estimation in the automotive industry. *Oil & Gas Science and Technology, 56*(4), 373-388.

Lyttle, A. D., Blanksby, B., Elliot, B., & Lloyd, D. G. (1998). The effect of depth and velocity on drag during the streamlined guide. *Journal of Swimming Research, 13*, 15-22.

Machtsiras, G. (2012). *Utilizing flow characteristics to increase performance in swimming.* (Doctor of Philosophy), The University of Edinburgh, Edinburgh, Scotland.

MacKinnon, D. P., Lockwood, C. M., & Williams, J. (2004). Confidence limits for the indirect effect: Distribution of the product and resampling methods. *Multivariate behavioral research, 39*(1), 99-128.

Marinho, D., Barbosa, T., Rouboa, A., & Silva, A. (2011). The hydrodynamic study of the swimming gliding: a two-dimensional computational fluid dynamics (CFD) analysis. *Journal of Human Kinetics, 29*, 49-57.

McCabe, C. B., & Sanders, R. H. (2012). Kinematic differences between front crawl sprint and distance swimmers at a distance pace. *Journal of sports sciences, 30*(6), 601-608.

Mollendorf, J. C., Albert, T., C, Oppenheim, E., & Pendergast, D. R. (2004). Effect of swim suit design on passive drag. *Medicine & Science in Sports & Exercise, 36*(6), 1029-1035.

Morais, J. E., Costa, M., Mejias, E., Marinho, D., Silva, A., & Barbosa, T. (2011). Morphometric study for estimation and validation of trunk transverse surface area to assess human drag force on water. *Journal of Human Kinetics, 28*, 5-13.

Morais, J. E., Jesus, S., Lopes, V., Garrido, N., Silva, A., Marinho, D., & Barbosa, T. M. (2012). Linking selected kinematic, anthropometric and hydrodynamic variables to young swimmer performance. *Pediatric Exercise Science, 24*(4), 649-664.

Morais, J. E., Jesus, S., Mejias, J. E., Costa, M. J., Moreira, M., Garrido, N. D., . . . Barbosa, T. M. (2013). Is the underwater gliding test a valid procedure to estimate the swimmers' drag? *International SportMed Journal*, *14*(4), 216-225.

Naemi, R., & Sanders, R. H. (2008). A “hydrokinematic” method of measuring the glide efficiency of a human swimmer. *Journal of biomechanical engineering, 130*(6).

Nicolas, G., Bideau, B., Colobert, B., & Berton, E. (2007). How are Strouhal number, drag, and efficiency adjusted in high level underwater monofin-swimming? *Human movement science, 26*(3), 426-442.

Papic, C., McCabe, C., Naemi, R., & Sanders, R. (2019). A method of quantifying torso shape to assess its influence on resistive drag in swimming. *ISBS Proceedings Archive, 37*(1), 113.

Pease, D., & Vennell, R. (2011). Comparison of wave drag for both the male and female form. *Proceedings of XXIX International Society of Biomechanics in Sports*, Porto, Portugal, 355-358.

Pendergast, D., Mollendorf, J., Zamparo, P., Termin 2nd, A., Bushnell, D., & Paschke, D. (2005). The influence of drag on human locomotion in water. *Undersea and Hyperbaric Medical Society, 32*(1), 45-57.

Psycharakis, S., Naemi, R., Connaboy, C., McCabe, C., & Sanders, R. (2010). Three-dimensional analysis of intracycle velocity fluctuations in frontcrawl swimming. *Scandinavian Journal of Medicine & Science in Sports, 20*(1), 128-135.

Seifert, L., Chollet, D., & Bardy, B. (2004). Effect of swimming velocity on arm coordination in the front crawl: a dynamic analysis. *Journal of sports sciences, 22*(7), 651-660.

Thow, J. L., Naemi, R., & Sanders, R. H. (2012). Comparison of modes of feedback on glide performance in swimming. *Journal of sports sciences, 30*(1), 43-52.

Toussaint, H., De Groot, G., Savelberg, H., Vervoorn, K., Hollander, A., & van Ingen Schenau, G. (1988). Active drag related to velocity in male and female swimmers. *Journal of biomechanics, 21*(5), 435-438.

555 Van der Vaart, A., Savelberg, H., De Groot, G., Hollander, A., Toussaint, H., & van Ingen
556 Schenau, G. (1987). An estimation of drag in front crawl swimming. *Journal of*
557 *biomechanics, 20*(5), 543-546.
558 Vilas-Boas, J. P., Costa, L., Fernandes, R. J., Ribeiro, J., Figueiredo, P., Marinho, D., . .
559 . Machado, L. (2010). Determination of the drag coefficient during the first and
560 second gliding positions of the breaststroke underwater stroke. *Journal of Applied*
561 *Biomechanics, 26*(3), 324-331.
562 Zamparo, P., Gatta, G., Pendergast, D., & Capelli, C. (2009). Active and passive drag:
563 the role of trunk incline. *European journal of applied physiology, 106*(2), 195-
564 205.
565

Tables

Table 1. Mean (standard deviation) torso shape and drag coefficient measurements for Group 1, Group 2 and Combined Cohort.

Outcome measure	**Group 1 (n = 15)**	**Group 2 (n = 10)**	***p***	**Combined (n = 25)**
Body mass (kg)	73.90 (8.73)	70.04 (6.63)	0.223	72.36 (8.04)
Torso length (m)	0.649 (0.026)	0.656 (0.030)	0.579	0.652 (0.988)
Cross sectional area (m^2)				
Chest	0.070 (0.009)	0.067 (0.007)	0.394	0.069 (0.008)
Waist	0.045 (0.005)	0.047 (0.006)	0.556	0.046 (0.005)
Hip	0.065 (0.006)	0.066 (0.007)	0.865	0.065 (0.006)
Rate of change in CSA (m^2/m)				
Chest-waist	-0.178 (0.046)	-0.171 (0.035)	0.694	-0.175 (0.413)
Waist-hip	0.214 (0.032)	0.204 (0.051)	0.591	0.210 (0.040)
Form gradients (m/m)				
Anterior chest-waist	-0.197 (0.109)	-0.220 (0.137)	0.662	-0.206 (0.119)
Anterior waist-hip	0.281 (0.149)	0.323 (0.105)	0.416	0.298 (0.132)
Posterior chest-waist	-0.337 (0.082)	-0.348 (0.150)	0.848	-0.341 (0.112)
Posterior waist-hip	0.597 (0.153)	0.504 (0.152)	0.152	0.560 (0.157)
Lateral (left) chest-waist	-0.298 (0.107)	-0.303 (0.080)	0.902	-0.300 (0.095)
Lateral (left) waist-hip	0.318 (0.070)	0.257 (0.072)	0.050	0.294 (0.076)
Lateral (right) chest-waist	-0.299 (0.071)	-0.294 (0.088)	0.883	-0.297 (0.077)
Lateral (right) waist-hip	0.250 (0.079)	0.277 (0.089)	0.453	0.260 (0.082)
Drag coefficient	3.18 (1.07)	2.62 (0.74)	0.133	2.96 (0.98)

570 Table 2. Pearson correlation coefficient between torso shape measurements and the drag

571 coefficient (n=25).

Torso shape measurements	***r***	***p***
Torso length (m)	-0.19	0.177
Body mass (kg)	-0.03	0.438
Cross sectional areas (m^2)		
Chest	0.01	0.475
Waist	0.23	0.134
Hip	0.16	0.222
Rate of change in cross-sectional area (m^2/m)		
Chest-waist	0.18	0.192
Waist-hip	0.44*	0.014
Form gradients (m/m)		
Anterior chest-waist	0.09	0.335
Anterior waist-hip	0.08	0.346
Posterior chest-waist	-0.16	0.217
Posterior waist-hip	0.50**	0.006
Lateral (left) chest-waist	0.23	0.132
Lateral (left) waist-hip	0.18	0.195
Lateral (right) chest-waist	0.32	0.060
Lateral (right) waist-hip	-0.16	0.224

572 * $p < 0.05$, ** $p < 0.01$

573

Figure captions

Figure 1. Maximum segment form gradient (m/m): Lateral (right) chest-waist (1–3) and waist-hip (3–5), lateral (left) chest-waist (2–4) and waist-hip (4–6), posterior chest-waist (7–9) and waist-hip (9–11), anterior chest-waist (8–10) and waist-hip (10–12).

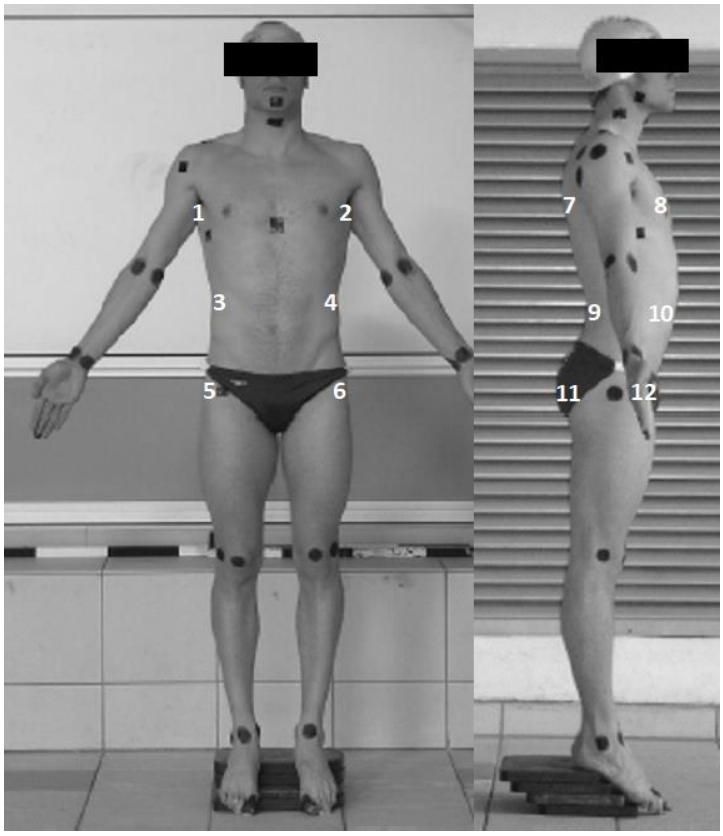

Figure 2. Maximum rate of change in cross sectional area waist-hip vs maximum drag coefficient.

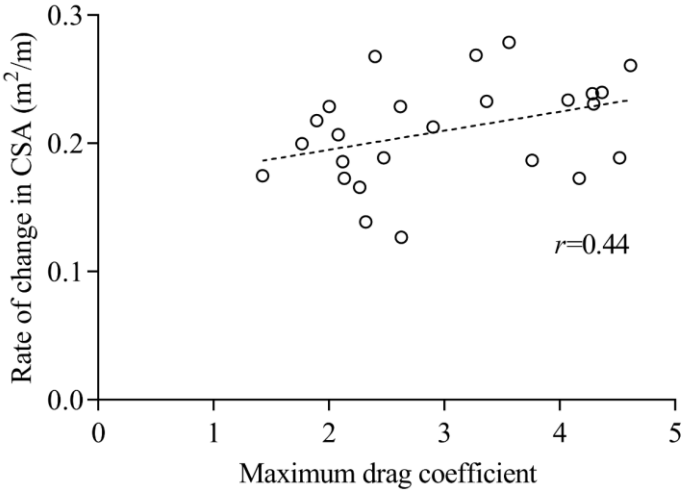

582 Figure 3. Maximum posterior form gradient waist-hip vs maximum drag coefficient.

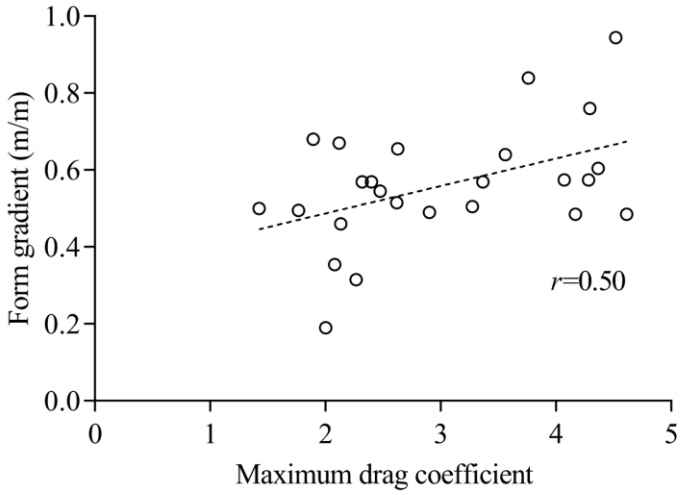

583